



# Short-Term Inhalation of Ultrafine Zinc Particles Could Alleviate Cardiac Dysfunctions in Rats of Myocardial Infarction

Li Li<sup>1</sup>, Pei Niu<sup>2</sup>, Xuan Wang<sup>1</sup>, Fangbo Bing<sup>1</sup>, Wenchang Tan<sup>1,2,3,4\*</sup> and Yunlong Huo<sup>5\*</sup>

<sup>1</sup> Department of Mechanics and Engineering Science, College of Engineering, Peking University, Beijing, China,

<sup>2</sup> PKU-HKUST Shenzhen-Hong Kong Institution, Shenzhen, China, <sup>3</sup> Peking University Shenzhen Graduate School,

Shenzhen, China, <sup>4</sup> Shenzhen Bay Laboratory, Shenzhen, China, <sup>5</sup> Institute of Mechanobiology and Medical Engineering, School of Life Sciences and Biotechnology, Shanghai Jiao Tong University, Shanghai, China

## OPEN ACCESS

### Edited by:

Rita Payan Carreira,  
University of Évora, Portugal

### Reviewed by:

Natalya Kizilova,  
Warsaw University of Technology,  
Poland

Cherry Lindsey Wainwright,  
Robert Gordon University,  
United Kingdom

### \*Correspondence:

Wenchang Tan  
tanwch@pku.edu.cn  
Yunlong Huo  
huoyunlong@sjtu.edu.cn

### Specialty section:

This article was submitted to  
Biomechanics,  
a section of the journal  
Frontiers in Bioengineering and  
Biotechnology

Received: 27 December 2020

Accepted: 25 March 2021

Published: 14 April 2021

### Citation:

Li L, Niu P, Wang X, Bing F, Tan W  
and Huo Y (2021) Short-Term  
Inhalation of Ultrafine Zinc Particles  
Could Alleviate Cardiac Dysfunctions  
in Rats of Myocardial Infarction.  
*Front. Bioeng. Biotechnol.* 9:646533.  
doi: 10.3389/fbioe.2021.646533

It is not clear for inhalation of ultrafine metal particles in air pollution to impair human health. In the study, we aimed to investigate whether short-term (4 weeks) inhalation of ultrafine zinc particles could deteriorate the cardiac and hemodynamic functions in rats of myocardial infarction (MI). MI was induced in Wistar rats through coronary artery ligation surgery and given an inhalation of ultrafine zinc particles for 4 weeks (post-MI 4 weeks, 4 days per week, and 4 h per day). Cardiac strain and strain rate were quantified by the speckle tracking echocardiography. The pressure and flow wave were recorded in the carotid artery and analyzed by using the Womersley model. Myocardial infarction resulted in the LV wall thinning, LV cavity dilation, remarkable decrease of ejection fraction, dp/dt Max,  $-dp/dt$  Min, myocardial strain and strain rates, and increased LV end-diastolic pressure, as well as impaired hemodynamic environment. The short-term inhalation of ultrafine zinc particles significantly alleviated cardiac and hemodynamic dysfunctions, which could protect from the MI-induced myocardial and hemodynamic impairments albeit it is unknown for the long-term inhalation.

**Keywords:** speckle-tracing echocardiography, strain analysis, ultrafine zinc particle, Womersley analysis, myocardium infarction

## INTRODUCTION

The adverse effects of ambient air pollution in the pathogenesis of acute and chronic diseases are recognized increasingly. The ultrafine metal particles in air pollution have the possibilities to deteriorate the cardiovascular diseases (Birmili et al., 2006; Kodavanti et al., 2008; Wallenborn et al., 2008). Zinc is one of the main metal elements in air pollution in China (Ming et al., 2017;

**Abbreviations:** HFpEF, Heart failure with preserved ejection fraction; HFrEF, Heart failure with reduced ejection fraction; STE, Speckle-tracing Echocardiography; BW, Body weight; HW, Heart weight; LV, Left ventricle; LAD, Left anterior descending artery; EF (%), Ejection fraction; FS (%), Fractional shortening; SV, Stroke volume; CO, Cardiac output; LVID;s, LV internal diameter in systole; LVID;d, LV internal diameter in diastole; ESV, End-systolic Volume of LV; EDV, End-diastolic Volume of LV; LVAW;s, LV Anterior wall in systole; LVAW;d, LV Anterior wall in diastole; LVPW;s, LV Posterior wall in systole; LVPW;d, LV Posterior wall in diastole; LVSP, LV systolic pressure; LVEDP, LV end-diastolic pressure; LCA, Left Carotid artery; SBP, Systolic blood pressure; DBP, Diastolic blood pressure; TAWSS, Time-average wall shear stress; OSI, Oscillating shear index; RRT, Relative residence time; WSS, Wall shear stress.

Du et al., 2019). Zinc is also a ubiquitous trace element. It is one of the most important and indispensable trace elements in the body, and it is involved in the growth and development of microorganisms, plants, and animals (Chasapis et al., 2012). Zinc ions ( $Zn^{2+}$ ) plays an important role in the excitation-contraction coupling of mammalian cardiomyocytes (Tuncay et al., 2011). Hence, it is worthwhile to study the effect of ultrafine zinc particles on cardiovascular diseases.

We have previously shown that the inhalation of ultrafine zinc particles deteriorated local myocardial dysfunctions in the LV and the hemodynamic environment in peripheral arteries in rats of hypertension-induced heart failure with preserved ejection fraction (HFpEF) (Bing et al., 2020). The zinc level increased in the blood and tissues of hypertensive rats after inhalation of zinc particles (Clegg et al., 1987; Leblondel and Allain, 1988; Henrotte et al., 1990). ZIP14 is a plasma membrane transporter that promotes extracellular zinc to enter the cytoplasm and increases the zinc concentration inside the cell (Taylor et al., 2005). Inhaling zinc particles upregulated zinc transporter ZIP14 expression (Huang J. Y. et al., 2018) and induced accumulation of intracellular  $Zn^{2+}$  in the myocytes, which resulted in the impaired excitation-contraction coupling of myocytes in hypertension-induced HFpEF (Macdonald, 2000; Murakami and Hirano, 2008). In contrast, a significant fall in serum zinc levels was observed in patients with acute myocardial infarction (MI) that induced heart failure with reduced ejection fraction (HFrEF) (Lewandowicz et al., 1979; Singh et al., 1983). Since there are totally different biological and hemodynamic mechanisms between HFpEF and HFrEF, we hypothesized that short-term inhalation of ultrafine zinc particles could slow down the progression of cardiac and hemodynamic impairments in rats of MI.

The objective of the study is to investigate cardiac and hemodynamic changes in rats of MI after inhaling ultrafine zinc particles. Wistar rats were selected for coronary artery ligation surgery to induce MI as well as inhalation of ultrafine zinc particles for 4 weeks. Physiological and hemodynamic measurements were carried out in the LV and carotid artery for 4 weeks after the ligation surgery. Speckle tracking echocardiography (STE) was used to analyze the ventricular functions (Voigt et al., 2015). The Womersley model was performed for the hemodynamic analysis in the carotid artery. The significance and implications of the study were discussed relevant to ultrafine zinc particles' protection effect on the MI-induced myocardial and hemodynamic impairments.

## MATERIALS AND METHODS

### Study Design

A total of 80 male 8-week-old Wistar rats (Beijing Vital River Laboratory Animal Technology Co., Ltd.), weighing  $208 \pm 14$  g, were used for this study. Rats were housed at standard SPF laboratory and free access to standard rodent chow and water. Randomly, 30 rats were divided into sham (sham group,  $n = 15$ ) and sham with inhalation of zinc particles (sham-Zn group,

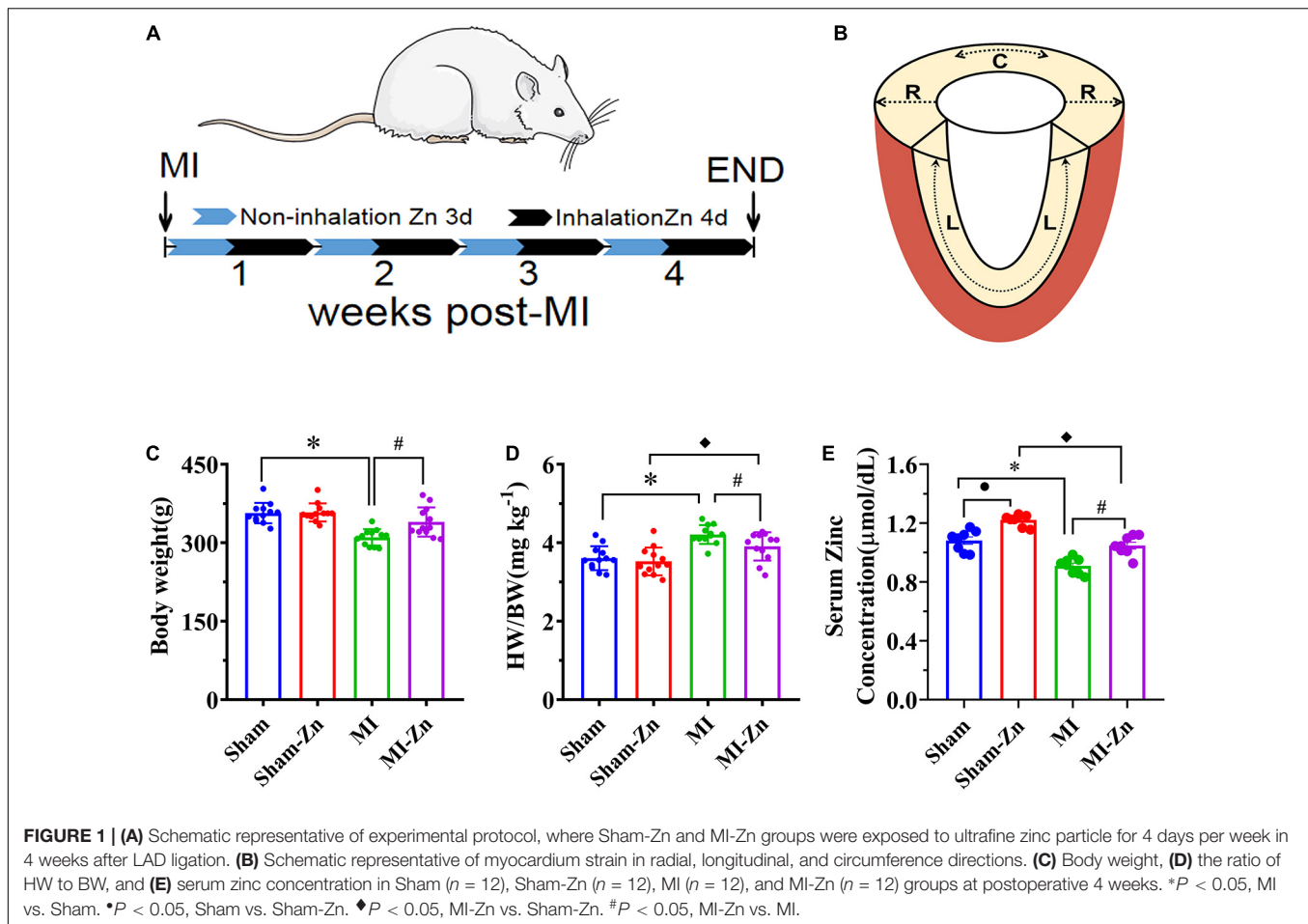
$n = 15$ ) and 50 rats were performed with left anterior descending artery (LAD) ligation surgery to induce MI. Six animals died during the surgery. Three days after surgery, half of the surviving MI rats ( $n = 22$ ) were exposed in the environment filled with ultrafine zinc particle (diameter of 50 nm and density of  $500 \mu\text{g}/\text{m}^3$ ) (MI-Zn group,  $n = 22$ ) using the same method as a previous study (Bing et al., 2020) while the rest were considered as the MI group ( $n = 22$ ). MI-Zn and Sham-Zn rats inhaled ultrafine zinc particles for 4 h per day and 4 days per week for 4 weeks, as shown in **Figure 1A**. All experiments were performed in accordance with Chinese National and Peking University ethical guidelines regarding the use of animals in research, consistent with the NIH guidelines (Guide for the care and use of laboratory animals) on protection of animals used for scientific purposes. The experimental protocol was approved by the Animal Care and Use Committee of Peking University, China.

### Myocardial Infarction

Left anterior descending artery ligation was performed in 50 Wistar rats. Briefly, in sterile environment, surgical anesthesia was maintained with  $\sim 2\%$  isoflurane and animals were intubated and ventilated with room air and oxygen using a Harvard ventilator (Inspira) (Niu et al., 2020). After the chest was shaved and sterilized, a left thoracotomy was performed between the third and fourth intercostal spaces. A 7-0 suture line was placed at 1 mm below the left auricle appendage to ligate the LAD artery, which led to pale LV anterior wall and apex region. Alternatively, the suture was placed but removed in sham-operated animals. After the chest was closed, animals were intramuscularly administered a dose of penicillin (400,000 U) and 1 ml dezocine (50  $\mu\text{g}/\text{ml}$ ) and allowed to recover from the surgery. Animals were given an intramuscular injection of penicillin (400,000 U) and 1 ml dezocine (50  $\mu\text{g}/\text{ml}$ ) for three consecutive days. All animals were cared at  $26^\circ\text{C}$  indoors, and under 12:12 h light/dark artificial cycle conditions for a total of 4 weeks after surgical recovery.

### Echocardiographic Measurements

Echocardiographic measurements of rat hearts, as shown in **Figure 1B**, were carried out under anesthesia for 4 weeks postoperatively. M-mode measurements of LV, left atrium, and aorta and B-mode measurements of strain and strain rate were recorded in rats, similar to a previous study (Niu et al., 2020). The images were obtained at 21 MHz using a MS-250 transducer operated by a Vevo 2100 Color Doppler Ultrasound Scanner (FUJIFILM VisualSonics Inc.). Based on M-mode tracings, morphometric parameters, e.g., LVID;d, LVID;s, LVFW;s, LVFW;d, IVS;s, and IVS;d, were measured according to the American Society of Echocardiography leading edge rule (Sahn et al., 1978). These parameters were averaged based on five measurements. Moreover, FS (%) and EF (%) were calculated from the measured parameters as:  $\frac{(LVID;d-LVID;s)}{LVID;d} \times 100\%$  and  $\frac{(LVID;d^3-LVID;s^3)}{LVID;d^3} \times 100\%$ , respectively, on a Vevo LAB image analysis workstation.



## STE Analysis

Myocardial deformation and movement measurements were carried out by using the Vevo LAB image analysis workstation with advanced STE, which tracks natural acoustic markers (called speckles) across the cardiac cycle and estimates velocity vectors. Strain measurement of myocardial deformation were obtained from B-Mode cine loops acquired from the parasternal long-axis and short-axis views (Niu et al., 2020). Frame rate is 133 Hz, gain is 20~25 dB, depth is ~20 mm, width is ~23 mm, and three cardiac cycles were recorded. Longitudinal and circumferential strains ( $S = \frac{\Delta L}{L_0}$ , where  $L_0$  and  $\Delta L$  refer to the baseline length at the R-Wave and the absolute change in length, respectively) and strain rate ( $SR = \frac{S}{\Delta t} = \frac{(\Delta L/L_0)}{\Delta t} = \frac{(\Delta L/\Delta t)}{L_0} = \frac{\Delta V}{L_0}$ , where  $\Delta V$  is the velocity gradient in the segment) were determined by the software across a selected period of cardiac cycles.

## Hemodynamic Measurements

The left carotid artery (LCA) was dissected in a sterile environment under anesthesia after the echocardiographic measurements. A perivascular flow probe (Transonic Systems Inc.; relative error of  $\pm 2\%$  at full scale) was used to measure volumetric flow rate of LCA. Moreover, a 1.4F micromanometer-tipped catheter (Millar Instruments) was inserted through the

right carotid artery into the LV to record pressure waves over 30 cardiac cycles, which was repeated three times. The zero-pressure baseline of the catheter was calibrated in the 37°C saline solution. The catheter and perivascular flow probe were monitored with a BIOPAC MP150. Heart rate, LV systolic pressure (LVSP), LV end-diastolic pressure (LVEDP), and rate of maximum positive and negative left ventricular pressure development ( $\frac{dp}{dt}_{max}$  and  $\frac{dp}{dt}_{min}$ ) were determined from the measured pressure waves.

## Serum Zinc Detection

After hemodynamic measurements, blood samples were taken from the tail vein and centrifuged at 3000 RPM for 15 min. The serum was extracted and stored at  $-20^\circ\text{C}$ . The Blood Zinc Concentration Detection Kit (Solarbio BC2815, Beijing Solarbio Science & Technology Co., Ltd.) was used to detect zinc concentration in the serum, which was measured by the microplate reader (Multiskan™ FC, Thermo Fisher Scientific, United States) with a wavelength of 620 nm.

## Histological Evaluation

All animals were terminated for the histological analysis at postoperative 4 weeks by intraperitoneal injection of 1% pentobarbital sodium at dose of 150 mg/kg (Niu et al., 2020).

After hearts were harvested, plugs of myocardial tissues were removed from different positions of the LV. These plugs were fixed in 4% paraformaldehyde (PFA)/PBS solution overnight at room temperature and then processed for paraffin sectioning. Masson's trichrome staining was carried out for determination of myocardial fibrosis according to standard procedures (Puente et al., 2014; Deng et al., 2016) while haematoxylin-eosin (HE) staining was performed to observe the arrangement and morphology of cardiomyocytes (Wu et al., 2017).

## Womersley Analysis

Similar to a previous study (Bing et al., 2020), the equation for the pulsatile flow velocity profile across the lumen,  $u(r, t)$ , is given as:

$$u(r, t) = \text{REAL} \left( \frac{2Q(0)(R^2 - r^2)}{\pi R^4} + \sum_{\omega=1}^{\infty} \frac{\frac{Q(\omega)}{\pi R^4} \cdot \left(1 - \frac{J_0(\Lambda r/R)}{J_0(\Lambda)}\right)}{1 - \frac{2J_1(\Lambda)}{\Lambda J_0(\Lambda)}} e^{i\omega t} \right) \quad (1)$$

where  $r$  is the radial coordinate,  $R$  is the radius of artery,  $\Lambda^2 = i^3 \alpha^2$ ,  $\alpha = R \sqrt{\frac{\omega \rho}{\mu}}$ ,  $q_{\text{measured}}(t) = Q(\omega) e^{i\omega t}$ ,  $\omega$  is the angular frequency after Fourier transformation,  $J_0$  is a Bessel function of zero order and first kind, and  $J_1$  is a Bessel function of first order and first kind. Accordingly, wall shear stress (WSS),  $\tau(R, t)$ , and oscillatory shear index (OSI) for pulsatile blood flow can be written as:

$$\tau(R, t) = \text{REAL} \left( \frac{4\mu}{\pi R^3} Q(0) - \sum_{\omega=1}^{\infty} \frac{\frac{\mu Q(\omega)}{\pi R^3} \cdot \frac{\Lambda J_1(\Lambda)}{J_0(\Lambda)}}{1 - \frac{2J_1(\Lambda)}{\Lambda J_0(\Lambda)}} \right) \quad (2)$$

$$\text{OSI} = \frac{1}{2} \left( 1 - \frac{\left| \frac{1}{T} \int_0^T \tau(R, t) dt \right|}{\frac{1}{T} \int_0^T |\tau(R, t)| dt} \right) \quad (3)$$

The viscosity ( $\mu$ ) and density ( $\rho$ ) were assumed to be 4.0 cp and 1.06 g/cm<sup>3</sup>, respectively. Moreover, relative residence time (RRT) reflects the residence time of flow particles near the wall and is recommended as a single metric of low oscillating shear stress, which is expressed as follows:

$$\text{RRT} = \frac{1}{(1 - 2 \cdot \text{OSI}) \cdot \text{TAWSS}} \quad (4)$$

## Statistical Analysis

The experimental measurements were repeated three times and averaged per animal. All parameters were represented as mean  $\pm$  S.E.M. by averaging over all animals in each group. A two-way ANOVA (SigmaStat 3.5) was used to detect the statistical difference of morphometric and hemodynamic parameters between sham and MI groups and between inhalation of zinc particle and no inhalation groups, where  $P < 0.05$  was indicative of a significant difference between the two populations.

## RESULTS

**Figures 1C,D** show the body weight and ratio of HW to BW in Sham, Sham-Zn, MI, and MI-Zn groups at postoperative 4 weeks, which shows no significant difference between Sham (BW: 357  $\pm$  20 g, HW/BW: 3.59  $\pm$  0.32) and Sham-Zn group (BW: 358  $\pm$  17 g, HW/BW: 3.54  $\pm$  0.37). MI-Zn rats have higher BW (340  $\pm$  28 g) and lower HW/BW (3.89  $\pm$  0.37) than the MI group (BW: 310  $\pm$  16 g, HW/BW: 4.21  $\pm$  0.25). The MI group has a significant decrease of BW and an increase of HW/BW than the Sham group and the MI-Zn group has higher HW/BW than the Sham-Zn group. Accordingly, **Figure 1E** shows the serum zinc concentration in the four groups. Myocardial infarction reduced the zinc concentration significantly while inhaling ultrafine zinc particle increased it.

**Table 1** lists morphometric and hemodynamic parameters in the heart of the four groups. There is no statistical difference between Sham and Sham-Zn groups except for LV wall thickness. In comparison with Sham and Sham-Zn groups, LVID;s, LVID;d, ESV, EDV, and LVEDP are significantly higher and LV free wall thickness and systolic and diastolic blood pressures are lower in MI and MI-Zn groups. On the other hand, the MI-Zn group has significantly higher systolic blood pressure and lower LV end-diastolic pressure than the MI group.

**Figure 2** shows EF, FS, LVEDP, Tau, dp/dt Max, and  $-dp/dt$  Min in four groups at postoperative 4 weeks, which have no statistical difference between Sham and Sham-Zn groups, but significant difference between Sham and MI groups and between Sham-Zn and MI-Zn groups. Moreover, the MI-Zn group has higher values of EF, FS, dp/dt Max, and  $-dp/dt$  Min and lower values of LVEDP and Tau as compared with the MI group.

**Figure 3** shows schematic representative of deformation analysis and long-axis and short-axis echocardiographic views in four groups. In comparison with Sham and Sham-Zn groups, peak values of longitudinal, circumferential, and radial strain and strain rates in both infarction and normal regions are significantly reduced in MI and MI-Zn groups, as shown in **Table 2**. There is no statistical difference of strain and strain rates between Sham and Sham-Zn groups. Peak values of longitudinal, circumferential and radial strain and strain rates in infarction and normal regions of MI and MI-Zn groups are significantly lower than those of Sham and Sham-Zn groups. While peak values of three directions' strain and strain rates in infarction and normal regions of the MI-Zn group are higher than those in the MI group.

**Figures 4A–D** show transient distribution of representative flow velocity in the carotid artery of four groups at postoperative 4 weeks. Accordingly, **Figures 4E–G** show mean values of TAWSS, OSI, and RRT. Sham-Zn and MI-Zn groups have higher TAWSS and lower RRT than the Sham and MI groups, respectively. The MI group has the highest OSI.

**Figures 5A,B** show HE and Masson trichromatic staining in the myocardium of four groups at postoperative 4 weeks. Accordingly, **Figure 5C** shows quantitative comparison of myocardium fibrosis between MI group and MI-Zn group. Myocardial infarction leads to a significant increase of

**TABLE 1** | Morphometric and hemodynamic parameter.

	Sham	Sham-Zn	MI	MI-Zn
SV ( $\mu$ l)	174 $\pm$ 70.0	187 $\pm$ 34.1	143 $\pm$ 20.4	170 $\pm$ 55.3
CO (ml/min)	65.0 $\pm$ 21.4	73.8 $\pm$ 17.4	48.9 $\pm$ 7.12	60.2 $\pm$ 29.2
LVID;s (mm)	3.42 $\pm$ 0.53	3.28 $\pm$ 0.41	9.17 $\pm$ 0.47*	8.84 $\pm$ 0.72# $\blacklozenge$
LVID;d (mm)	6.29 $\pm$ 0.43	6.66 $\pm$ 0.54	10.4 $\pm$ 0.82*	9.98 $\pm$ 0.73 $\blacklozenge$
ESV ( $\mu$ l)	50.0 $\pm$ 17.7	43.5 $\pm$ 13.5	468 $\pm$ 53.0*	396 $\pm$ 74.7# $\blacklozenge$
EDV ( $\mu$ l)	202 $\pm$ 30.7	230 $\pm$ 43.1	618 $\pm$ 107*	566 $\pm$ 91.3 $\blacklozenge$
LVAW;s (mm)	2.56 $\pm$ 0.30	2.97 $\pm$ 0.12*	1.07 $\pm$ 0.11*	1.15 $\pm$ 0.42 $\blacklozenge$
LVAW;d (mm)	1.67 $\pm$ 0.14	1.92 $\pm$ 0.05*	1.03 $\pm$ 0.11*	1.19 $\pm$ 0.39 $\blacklozenge$
LVPW;s (mm)	2.50 $\pm$ 0.24	3.01 $\pm$ 0.21*	2.56 $\pm$ 0.37	2.60 $\pm$ 0.57
LVPW;d (mm)	1.67 $\pm$ 0.18	2.02 $\pm$ 0.18*	1.91 $\pm$ 0.25*	1.95 $\pm$ 0.26
LVSP (mmHg)	124 $\pm$ 14.7	127 $\pm$ 11.4	101 $\pm$ 23.63*	110 $\pm$ 11.9 $\blacklozenge$
LVEDP (mmHg)	1.29 $\pm$ 0.88	3.62 $\pm$ 4.01	17.8 $\pm$ 9.68*	10.1 $\pm$ 4.78# $\blacklozenge$
SBP (mmHg)	134 $\pm$ 15.2	140 $\pm$ 5.32	106 $\pm$ 6.34*	114 $\pm$ 4.99# $\blacklozenge$
DBP (mmHg)	100 $\pm$ 16.2	116 $\pm$ 6.98	86 $\pm$ 11.0*	89.3 $\pm$ 8.83

\* $P < 0.05$ , Sham vs. Sham-Zn, \* $P < 0.05$ , MI vs. Sham,  $\blacklozenge P < 0.05$ , Sham-Zn vs. MI-Zn, and # $P < 0.05$ , MI-Zn vs. MI.

myocardium fibrosis, which is inhibited by short-term inhalation of ultrafine zinc particles.

## DISCUSSION

This study investigated the effects of inhaling ultrafine zinc particles on cardiac function and peripheral cardiovascular hemodynamics in normal and MI animals experimentally and theoretically. The findings revealed that short-term inhalation of ultrafine zinc particles could inhibit the progression of the MI-induced heart failure.

### LV Dysfunctions and Remodeling

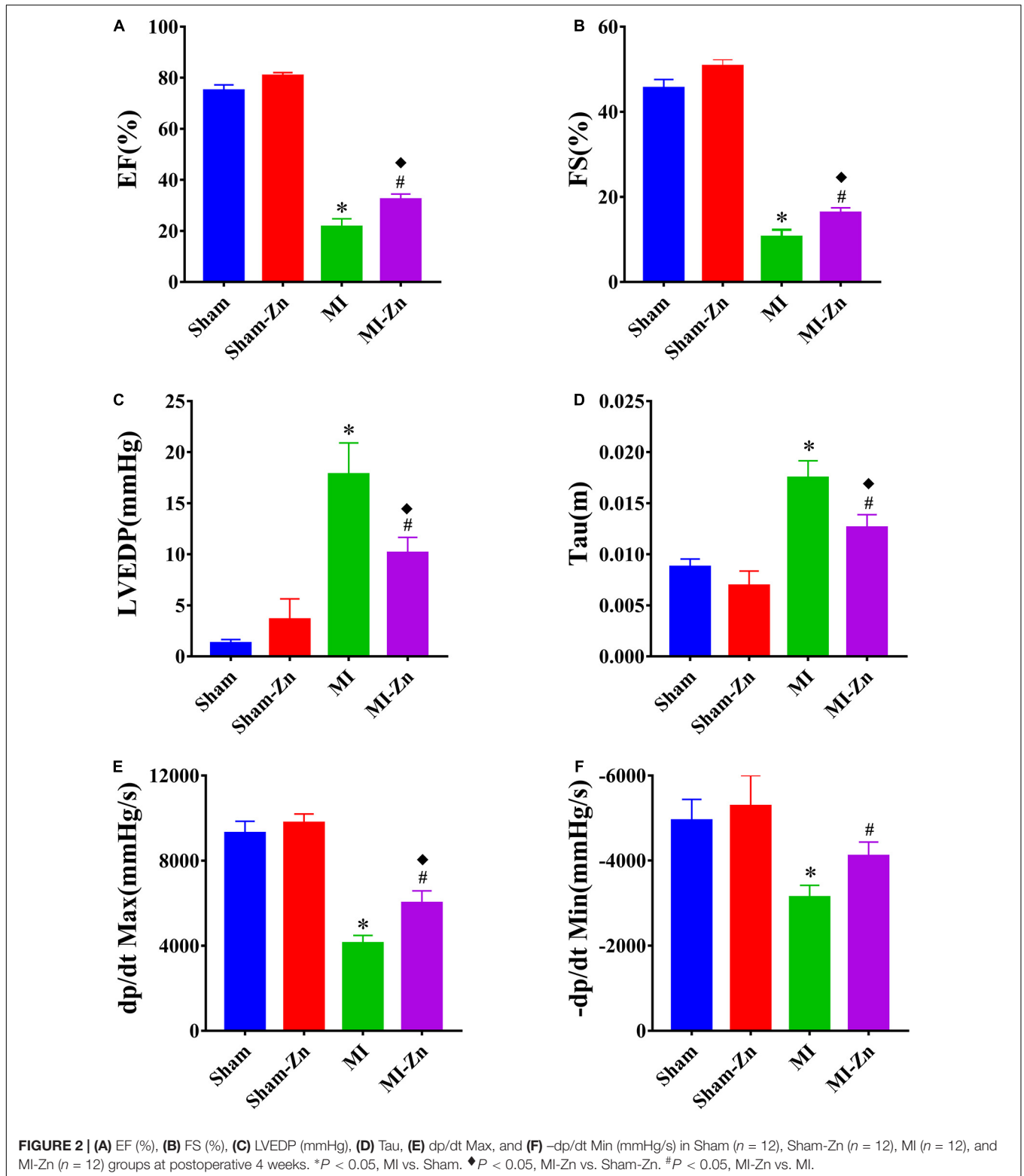
Myocardial infarction resulted in cardiac impairments, such as LV wall thinning, LV cavity dilation, remarkable decrease of EF, FS, dp/dt Max, and  $-dp/dt$  Min, and increased LVEDP and Tau as well as decreased systolic and diastolic blood pressures for 4 weeks after LAD ligation. The short-term inhalation of ultrafine zinc particles slowed down cardiac impairments caused by the myocardial infarction. The role of zinc as a modulator of cardiac changes has been recognized, which could affect homeostasis, oxidative stress, immune function, apoptosis, and ageing (Chasapis et al., 2012; Andrea et al., 2018). Zinc, a vital antioxidative element, can protect myocyte membrane against unsaturated lipids and inflammatory cytokines (Hennig et al., 1996) and thus alleviate the infarction-induced heart failure (Shokrzadeh et al., 2009) albeit there was much debate about the role of zinc concentrations in different types of cardiomyopathy (Marin and Rodriguez-Martinez, 1995; Kosar et al., 2006). A meta-analysis indicated a significant association between zinc deficiency and MI (Liu et al., 2015). The short-term inhalation of ultrafine zinc particles alleviated myocardial dysfunctions and slowed down conversion of MI to heart failure in MI rats, which agreed with previous studies that EF increased with Zn content (Oster et al., 1993) and Zn supplementation to a cardioplegic solution reversed the loss of systolic function (Powell et al., 1995).

Myocardial fibrosis makes a critical contribution to the LV remodeling in MI-induced HFReEF. Ultrafine zinc particles entered the systemic circulation through the respiratory system and suppressed tissue collagen deposition by inhibiting proline hydroxylase activity (Mezey et al., 1976; Mann et al., 1979; Camps et al., 1992), and regulated metabolism of fiber collagen (Wang et al., 2005). Wang et al. (2005) have shown that myocardial fibrosis was related to metallothionein (MT) regulation of zinc homeostasis and zinc supplementation prevented the fibrotic process in the MT-KO mice. Inhaling ultrafine zinc particles reduced the degree of myocardial fibrosis and hence slowed down conversion of MI to heart failure in MI rats.

The MI group had a significant decrease of systolic and diastolic blood pressures. The short-term inhalation of ultrafine zinc particles stimulated peripheral arteries and arterioles to elevate systolic and diastolic blood pressures in the MI-Zn group, which can be another factor for Zn protection against the MI-induced heart failure. On the other hand, we have shown a significant increase of systolic and diastolic blood pressures in rats of HFpEF (Bing et al., 2020). The short-term inhalation of ultrafine zinc particles further increased the systolic and diastolic blood pressures and hence deteriorated cardiac and hemodynamic environment in rats with HFpEF.

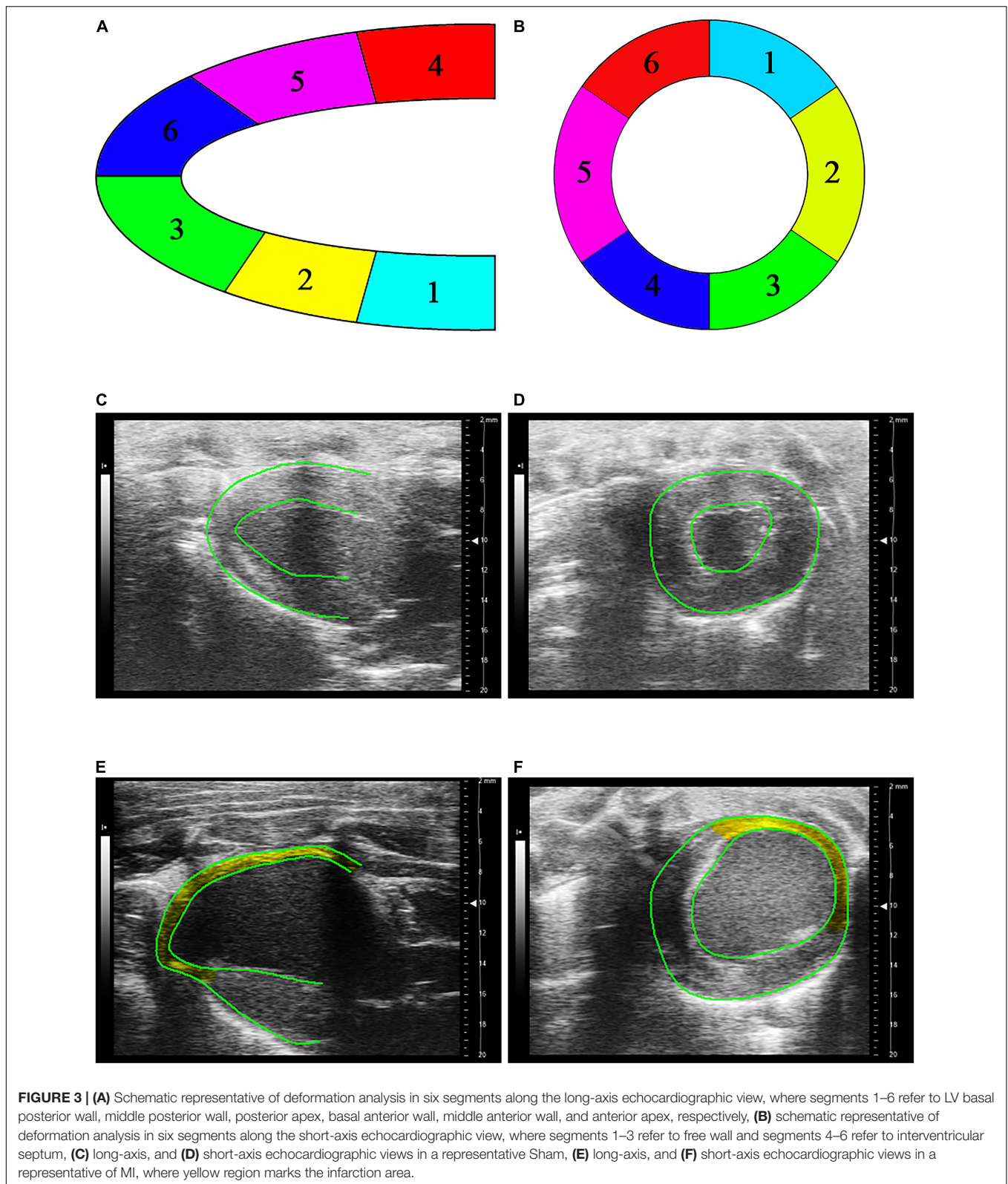
### Cardiac Strain Analysis

Myocardial strain and strain rate characterize the extent of cardiac deformation (Niu et al., 2020). In the STE analysis, the longitudinal strain refers to the shortening of myocardium fibers from the base to the apex, the circumferential strain represents the circumferential shortening observed in the short-axis view (Saito et al., 2009), and the radial strain shows the myocardial shortening moving from the LV center to the periphery (Heimdal, 1998). Accordingly, the strain rates refer to the relaxation of myocardium fibers (Niu et al., 2020). The MI-induced decrease of longitudinal, circumferential and radial strains and strain rates denoted the significant impairment of systolic and diastolic functions, respectively. The short-term inhalation of ultrafine



zinc particles slowed down the progression of systolic and diastolic dysfunctions. In mammalian myocytes, it is known that  $Zn^{2+}$  is of importance to regulate the excitation-contraction coupling (Turan et al., 1997; Tuncay et al., 2011). Woodier and

co-workers showed that cytosolic  $Zn^{2+}$  acted as a high affinity activator of RyR2 and modulated the frequency and amplitude of  $Ca^{2+}$  waves in myocytes in a concentration-dependent manner (Woodier et al., 2015). Defective  $Zn^{2+}$  handling enhanced the



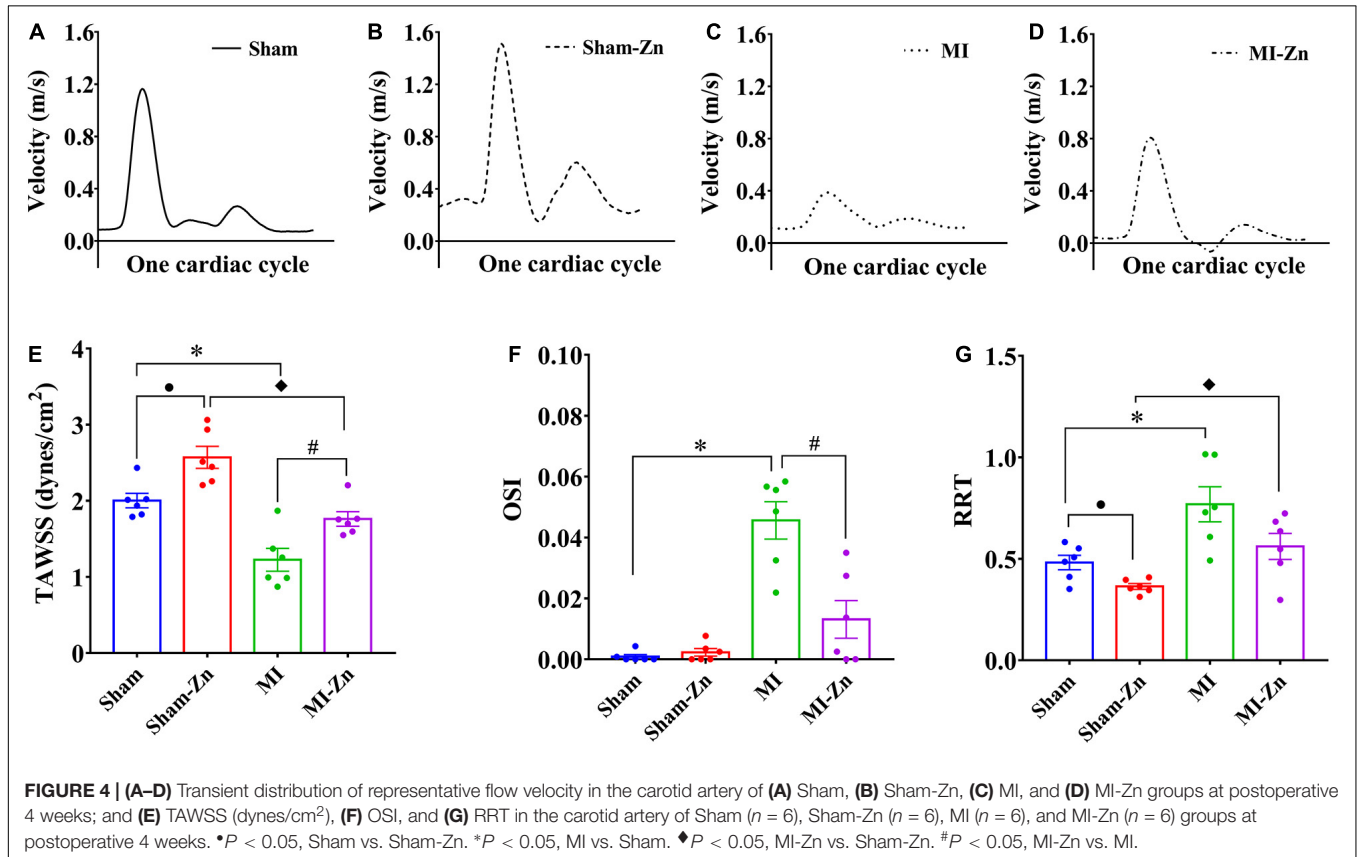
impaired contractility in myocytes (Little et al., 2010). Inhaling ultrafine zinc particles significantly increased the serum zinc concentration. Zinc transporter Zip14 can transfer the elevated

extracellular zinc into cardiomyocytes (Taylor et al., 2005; Kim et al., 2017; Yusuf et al., 2018) to alleviate systolic and diastolic dysfunctions in MI rats.

**TABLE 2** | Myocardial strain and strain rate derived by echocardiography.

	Normal zone				Infraction zone			
	Sham	Sham-Zn	MI	MI-Zn	Sham	Sham-Zn	MI	MI-Zn
L-Strain	-18.16 ± 2.57	-19.75 ± 4.27	-7.39 ± 4.29*	-11.19 ± 3.75♦#	-15.36 ± 2.99	-15.12 ± 3.56	-4.55 ± 1.95*	-5.27 ± 2.27♦
L-Strain rate	-4.15 ± 0.72	-4.85 ± 1.45	-2.52 ± 0.86*	-3.15 ± 0.51♦#	-3.25 ± 0.67	-3.77 ± 0.96	-1.57 ± 0.42*	-1.86 ± 0.52♦
C-Strain	-22.06 ± 3.35	-22.12 ± 6.86	-10.09 ± 5.00*	-14.90 ± 3.99♦#	-19.57 ± 5.03	-18.80 ± 6.42	-2.83 ± 2.35*	-7.97 ± 2.50♦#
C-Strain rate	-4.86 ± 0.84	-5.91 ± 2.16	-2.64 ± 0.84*	-3.48 ± 1.03♦#	-4.47 ± 1.45	-4.81 ± 1.37	-1.21 ± 0.43*	-1.60 ± 0.34♦#
R-Strain	41.51 ± 6.29	39.21 ± 16.35	14.21 ± 7.23*	27.95 ± 3.65♦#	32.95 ± 9.42	39.46 ± 9.93	7.31 ± 5.06*	20.55 ± 5.26♦#
R-Strain rate	6.02 ± 0.82	6.35 ± 1.16	3.93 ± 0.76*	5.20 ± 0.86♦#	5.48 ± 1.17	6.78 ± 1.59	3.13 ± 1.11*	4.45 ± 1.24♦#

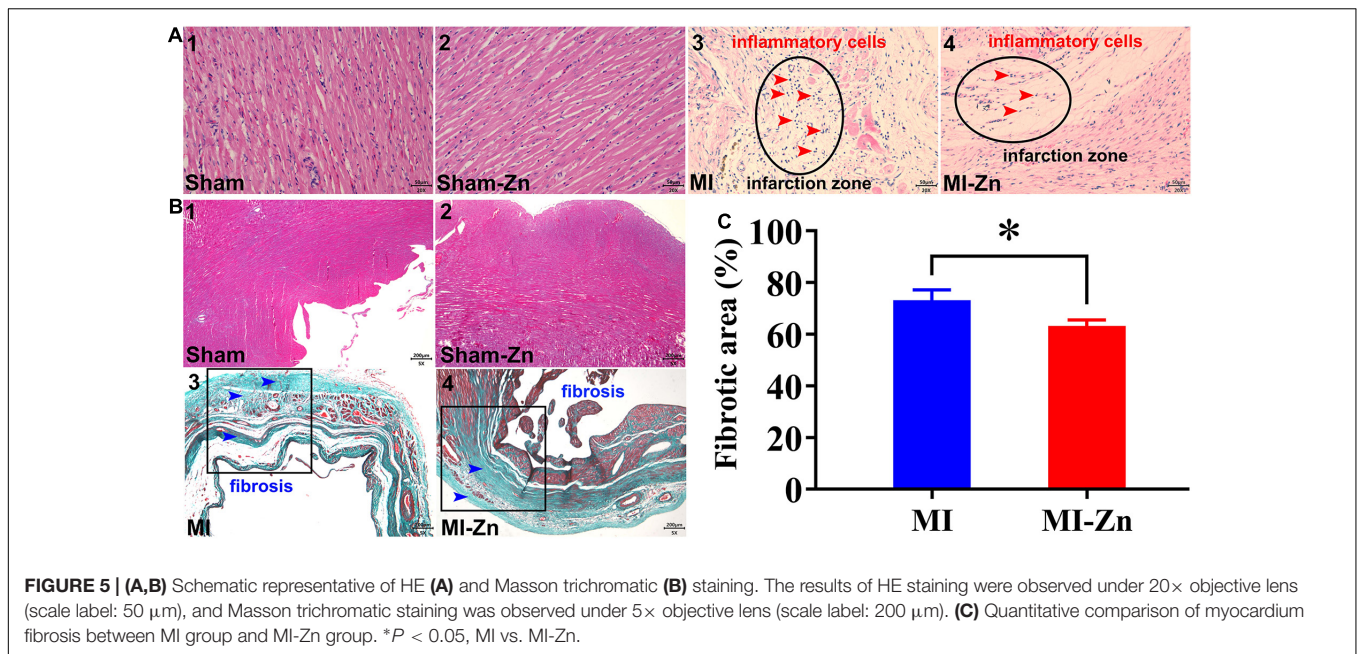
L, Longitudinal; C, Circumferential; R, Radial. \* $P < 0.05$ , MI vs. Sham; ♦ $P < 0.05$ , Sham-Zn vs. MI-Zn; # $P < 0.05$ , MI-Zn vs. MI.



## Hemodynamics in Peripheral Arteries

We investigated the hemodynamic changes in the carotid artery of the four groups. The Womersley analysis showed ~39% reduction of TAWSS in the MI group as compared with the shams. TAWSS in the Sham-Zn group was ~28% higher than that in the Sham group while the value in the MI-Zn group was ~44% higher than that in the MI group. This was caused by the increased CO and SV after short-term inhalation of ultrafine zinc particles. Moreover, OSI is high in the MI group despite negligible values in other groups. RRT in the MI group was ~60% higher than the shams while the value in the MI-Zn group was ~27% lower than that in MI group. The short-term inhalation of ultrafine zinc particles alleviated the hemodynamic environment

in the carotid artery, such as the increased TAWSS, the decreased OSI, and the reduced RRT. These abnormal parameters are known to result in endothelial dysfunction, monocyte deposition, SMC proliferation, microemboli formation, and so on (Huang et al., 2016; Han et al., 2018; Huang X. et al., 2018; Fan et al., 2019). It was reported that MI-induced zinc deficiency aggravates pro-inflammatory and impairs anti-inflammatory responses in vascular endothelial cells through activation of NF- $\kappa$ B and inhibition of PPAR pathways (Connell et al., 1997; Li and Karin, 1999; Chung et al., 2000; Delerive et al., 2000; Hihi et al., 2002; Griendling and FitzGerald, 2003). Zinc supplementation could function as the anti-inflammatory (Jarosz et al., 2017), preventing endothelial cell dysfunction, and subsequent cardiovascular



diseases (Shen, 2008). Hence, the short-term inhalation of ultrafine zinc particles may protect peripheral arteries from the hemodynamic impairments, which still required more investigations.

### Critique of the Study

We only measured the serum zinc levels, but not the concentration in myocardial tissues. The proportion of serum zinc entering cardiomyocyte via zinc transporter Zip14 is required to be investigated in the following studies. A further limitation is the lack of inclusion of a control particle, for example, an inert particle of the same size which is identified harmless to body. This is essential to demonstrate that the effects are down to zinc *per se*, rather than simply particulate matter. The present study only considered the effects of short-term inhalation on cardiac function and peripheral cardiovascular hemodynamics. The long-term inhalation of ultrafine zinc particles should be included in the following studies. Moreover, histological analysis and cellular and molecular mechanisms are still required for investigations.

### CONCLUSION

Myocardial infarction induced cardiac and hemodynamic impairments. The short-term inhalation of ultrafine zinc particles increased EF, FS, cardiac strain, and strain rate as well as decreased LVEDP, which slowed down myocardial dysfunctions in rats of MI. Moreover, the short-term inhalation of ultrafine zinc particles increased TAWSS and decreased OSI and RRT and hence protected peripheral arteries from the hemodynamic impairments.

### DATA AVAILABILITY STATEMENT

The original contributions presented in the study are included in the article/supplementary material, further inquiries can be directed to the corresponding authors.

### ETHICS STATEMENT

The animal study was reviewed and approved by the Animal Care and Use Committee of Peking University.

### AUTHOR CONTRIBUTIONS

LL and PN participated in the design of the study and carried out the animal lab work. LL carried out data statistics analysis and drafted the manuscript. XW and FB carried out the Womersley analysis. WT and YH critically revised the manuscript and conceived and designed the study. All authors contributed to the article and approved the submitted version.

### FUNDING

This work was supported by the National Natural Science Foundation of China Grant 11732001 (WT and YH), Shenzhen Science and Technology R&D Grant KQTD20180411143400981 (WT and YH), and Leading Talents Program of Guangdong Province 2016LJ06S686 (WT).

### ACKNOWLEDGMENTS

We would like to thank Fatiesa Sulejmani for valuable discussions about simulation.

## REFERENCES

- Andrea, F. G., Bertha, F. P., and Fernandes, A. A. (2018). Zinc supplementation attenuates cardiac remodeling after experimental myocardial infarction. *Cell. Physiol. Biochem.* 50, 353–362. doi: 10.1159/000494011
- Bing, F., Wang, X., Shen, W., Li, L., Niu, P., Chen, Y., et al. (2020). Inhalation of ultrafine zinc particles impaired cardiovascular functions in hypertension-induced heart failure rats with preserved ejection fraction. *Front. Bioeng. Biotechnol.* 8:13. doi: 10.3389/fbioe.2020.00013
- Birmili, W., Allen, A. G., Bary, F., and Harrison, R. M. (2006). Trace metal concentrations and water solubility in size-fractionated atmospheric particles and influence of road traffic. *Environ. Sci. Technol.* 40, 1144–1153. doi: 10.1021/es0486925
- Camps, J., Bargallo, T., Gimenez, A., Alie, S., Caballeria, J., Pares, A., et al. (1992). Relationship between hepatic lipid peroxidation and fibrogenesis in carbon tetrachloride-treated rats: effect of zinc administration. *Clin. Sci.* 83, 695–700. doi: 10.1042/cs0830695
- Chasapis, C. T., Loutsidou, A. C., Spiliopoulou, C. A., and Stefanidou, M. E. (2012). Zinc and human health: an update. *Arch. Toxicol.* 86, 521–534. doi: 10.1007/s00204-011-0775-1
- Chung, S. W., Kang, B. Y., Kim, S. H., Pak, Y. K., Cho, D., Trinchieri, G., et al. (2000). Oxidized low density lipoprotein inhibits interleukin-12 production in lipopolysaccharide-activated mouse macrophages via direct interactions between peroxisome proliferator-activated receptor- $\gamma$  and nuclear factor- $\kappa$  B. *J. Biol. Chem.* 275, 32681–32687. doi: 10.1074/jbc.M002577200
- Clegg, M. S., Ferrell, F., and Keen, C. L. (1987). Hypertension-induced alterations in copper and zinc metabolism in Dahl rats. *Hypertension* 9, 624–628. doi: 10.1161/01.hyp.9.6.624
- Connell, P., Young, V. M., Toborek, M., Cohen, D. A., Barve, S., McClain, C. J., et al. (1997). Zinc attenuates tumor necrosis factor-mediated activation of transcription factors in endothelial cells. *J. Am. Coll. Nutr.* 16, 411–417. doi: 10.1080/07315724.1997.10718706
- Delivero, P., Gervois, P., Fruchart, J. C., and Staels, B. (2000). Induction of I $\kappa$ B $\alpha$  expression as a mechanism contributing to the anti-inflammatory activities of peroxisome proliferator-activated receptor- $\alpha$  activators. *J. Biol. Chem.* 275, 36703–36707. doi: 10.1074/jbc.M004045200
- Deng, K. Q., Wang, A., Ji, Y. X., Zhang, X. J., Fang, J., Zhang, Y., et al. (2016). Suppressor of IKK $\alpha$  is an essential negative regulator of pathological cardiac hypertrophy. *Nat. Commun.* 7:11432.
- Du, L., Yan, W., Zhicheng, W., Chenxiao, H., and Huiting, M. (2019). PM<sub>2.5</sub>-bound toxic elements in an Urban City in East China: concentrations, sources, and health risks. *Int. J. Environ. Res. Public Health* 16:164. doi: 10.3390/ijerph16010164
- Fan, T., Zhou, Z., Fang, W., Wang, W., Xu, L., and Huo, Y. (2019). Morphometry and hemodynamics of coronary artery aneurysms caused by atherosclerosis. *Atherosclerosis* 284, 187–193. doi: 10.1016/j.atherosclerosis.2019.03.001
- Griendling, K. K., and FitzGerald, G. A. (2003). Oxidative stress and cardiovascular injury: part II: animal and human studies. *Circulation* 108, 2034–2040. doi: 10.1161/01.CIR.0000093661.90582.c4
- Han, Y., Huang, K., Yao, Q. P., and Jiang, Z. L. (2018). Mechanobiology in vascular remodeling. *Nat. Sci. Rev.* 5, 933–946. doi: 10.1093/nsr/nwx153
- Heimdal, A. (1998). Real-time strain rate imaging of the left ventricle by ultrasound. *J. Am. Soc. Echocardiogr.* 11, 1013–1019. doi: 10.1016/s0894-7317(98)70151-8
- Hennig, B., Toborek, M., and McClain, C. J. (1996). Antiatherogenic properties of zinc: implications in endothelial cell metabolism. *Nutrition* 12, 711–717. doi: 10.1016/s0899-9007(96)00125-6
- Henrotte, J. G., Santarromana, M., Franck, G., and Bourdon, R. (1990). Blood and tissue zinc levels in spontaneously hypertensive rats. *J. Am. Coll. Nutr.* 9, 340–343. doi: 10.1080/07315724.1990.10720390
- Hibi, A. K., Michalik, L., and Wahli, W. (2002). PPARs: transcriptional effectors of fatty acids and their derivatives. *Cell. Mol. Life Sci.* 59, 790–798. doi: 10.1007/s00018-002-8467-x
- Huang, J. Y., Teng, T. M., Bian, B., Du, L. P., Sun, Y. M., and Yang, Q. (2018). Cardiac zinc accumulation and endoplasmic reticulum stress in rats with ejection fraction preserved heart failure. *Chin. J. Misdiagn.* 13, 149–156.
- Huang, X., Liu, D., Yin, X., E, Y., Li, Z., Tan, W., et al. (2018). Morphometry and hemodynamics of posterior communicating artery aneurysms: ruptured versus unruptured. *J. Biomech.* 76, 35–44. doi: 10.1016/j.jbiomech.2018.05.019
- Huang, X., Yin, X., Xu, Y., Jia, X., Li, J., Niu, P., et al. (2016). Morphometric and hemodynamic analysis of atherosclerotic progression in human carotid artery bifurcations. *Am. J. Physiol. Heart Circ. Physiol.* 310, H639–H647.
- Jarosz, M., Wyszogrodzka, G., Librowski, T., Olbert, M., and Młyniec, K. (2017). Antioxidant and anti-inflammatory effects of zinc. Zinc-dependent NF- $\kappa$ B signaling. *Inflammopharmacology* 25, 11–24. doi: 10.1007/s10787-017-0309-4
- Woodier, J., Rainbow, R. D., Stewart, A. J., and Pitt, S. J. (2015). Intracellular zinc modulates cardiac ryanodine receptor-mediated calcium release. *J. Biol. Chem.* 290, 17599–17610. doi: 10.1074/jbc.m115.661280
- Kodavanti, U. P., Schladweiler, M. C., Gilmour, P. S., Wallenborn, J. G., Mandavilli, B. S., Ledbetter, A. D., et al. (2008). The role of particulate matter-associated zinc in cardiac injury in rats. *Environ. Health Perspect.* 116, 13–20. doi: 10.1289/ehp.10379
- Kosar, F., Sahin, I., Taskapan, C., Kucukbay, Z., Gullu, H., Taskapan, H., et al. (2006). Trace element status (Se, Zn, Cu) in heart failure. *Anadolu Kardiyol. Derg.* 6, 216–220.
- Leblondel, G., and Allain, P. (1988). Altered element concentrations in tissues of spontaneously hypertensive rats. *Biomed. Pharmacother.* 42, 121–129.
- Lewandowicz, J., Komorowski, J. M., and Goliński, H. (1979). Metabolic disorders in myocardial infarction. Changes of blood serum zinc, growth hormone, insulin and glucose concentration in patients with acute myocardial infarction. *Cor Vasa* 21, 305–316.
- Li, N., and Karin, M. (1999). Is NF- $\kappa$ B the sensor of oxidative stress? *FASEB J.* 13, 1137–1143.
- Little, P. J., Bhattacharya, R., Moreyra, A. E., and Korichneva, I. L. (2010). Zinc and cardiovascular disease. *Nutrition* 26, 1050–1057. doi: 10.1016/j.nut.2010.03.007
- Liu, B., Cai, Z. Q., and Zhou, Y. M. (2015). Deficient zinc levels and myocardial infarction. *Biol. Trace Element Res.* 165, 41–50. doi: 10.1007/s12011-015-0244-4
- Macdonald, R. S. (2000). The role of zinc in growth and cell proliferation. *J. Nutr.* 130(S5 Suppl):1500S. doi: 10.1093/jn/130.5.1500s
- Mann, S. W., Fuller, G. C., Rodil, J. V., and Vidins, E. I. (1979). Hepatic prolyl hydroxylase and collagen synthesis in patients with alcoholic liver disease. *Gut* 20, 825–832. doi: 10.1136/gut.20.10.825
- Marin, J., and Rodriguez-Martinez, M. A. (1995). Nitric oxide, oxygen-derived free radicals and vascular endothelium. *J. Auton. Pharmacol.* 15, 279–307. doi: 10.1111/j.1474-8673.1995.tb00311.x
- Mezey, E., Potter, J. J., and Maddrey, W. C. (1976). Hepatic collagen proline hydroxylase activity in alcoholic liver disease. *Clin. Chim. Acta* 68, 313–320. doi: 10.1016/0009-8981(76)90397-1
- Kim, M. H., Aydemir, T. B., Kim, J., and Cousins, R. J. (2017). Hepatic ZIP14-mediated zinc transport is required for adaptation to endoplasmic reticulum stress. *Proc. Natl. Acad. Sci. U.S.A.* 114:E5805.
- Ming, L., Jin, L., Li, J., Fu, P., Yang, W., Liu, D., et al. (2017). PM<sub>2.5</sub> in the Yangtze River Delta, China: chemical compositions, seasonal variations, and regional pollution events. *Environ. Pollut.* 223, 200–212. doi: 10.1016/j.envpol.2017.01.013
- Murakami, M., and Hirano, T. (2008). Intracellular zinc homeostasis and zinc signaling. *Cancer Sci.* 99, 1515–1522. doi: 10.1111/j.1349-7006.2008.00854.x
- Niu, P., Li, L., Yin, Z., Du, J., Tan, W., and Huo, Y. (2020). Speckle tracking echocardiography could detect the difference of pressure overload-induced myocardial remodeling between young and adult rats. *J. R. Soc. Interface* 17:20190808. doi: 10.1098/rsif.2019.0808
- Yusuf, O., Ozdemir, S., and Turan, B. (2018). Induction of endoplasmic reticulum stress and changes in expression levels of Zn<sup>2+</sup>-transporters in hypertrophic rat heart. *Mol. Cell. Biochem. Int. J. Chem. Biol.* 440, 209–219. doi: 10.1007/s11010-017-3168-9
- Oster, O., Dahm, M., and Oelert, H. (1993). Element concentrations (selenium, copper, zinc, iron, magnesium, potassium, phosphorous) in heart tissue of patients with coronary heart disease correlated with physiological parameters of the heart. *Eur. Heart J.* 14, 770–774. doi: 10.1093/eurheartj/14.6.770
- Powell, S. R., Aiuto, L., Hall, D., and Tortolani, A. J. (1995). Zinc supplementation enhances the effectiveness of St. Thomas' Hospital No. 2 cardioplegic solution

- in an in vitro model of hypothermic cardiac arrest. *J. Thorac. Cardiovasc. Surg.* 110, 1642–1648. doi: 10.1016/s0022-5223(95)70025-0
- Puente, B. N., Kimura, W., Muralidhar, S. A., Moon, J., Amatruda, J. F., Phelps, K. L., et al. (2014). The oxygen-rich postnatal environment induces cardiomyocyte cell-cycle arrest through DNA damage response. *Cell* 157, 565–579. doi: 10.1016/j.cell.2014.03.032
- Sahn, D. J., DeMaria, A., Kisslo, J., and Weyman, A. (1978). Recommendations regarding quantitation in M-mode echocardiography: results of a survey of echocardiographic measurements. *Circulation* 58, 1072–1083. doi: 10.1161/01.cir.58.6.1072
- Saito, K., Okura, H., Watanabe, N., Hayashida, A., Obase, K., Imai, K., et al. (2009). Comprehensive evaluation of left ventricular strain using speckle tracking echocardiography in normal adults: comparison of three-dimensional and two-dimensional approaches. *J. Am. Soc. Echocardiogr.* 22, 1025–1030. doi: 10.1016/j.echo.2009.05.021
- Shen, H. (2008). *Zinc Deficiency and Mechanisms of Endothelial Cell Dysfunction*. University of Kentucky Doctoral Dissertations. 610.
- Shokrzadeh, M., Ghaemian, A., Salehifar, E., Aliakbari, S., Saravi, S. S., and Ebrahimi, P. (2009). Serum zinc and copper levels in ischemic cardiomyopathy. *Biol. Trace Elem. Res.* 127, 116–123. doi: 10.1007/s12011-008-8237-1
- Singh, R., Mehrotra, M. P., Singh, M. M., Jain, V. K., and Kumar, P. (1983). Serum zinc in myocardial infarction: diagnostic and prognostic significance. *Angiology* 34, 215–221. doi: 10.1177/000331978303400308
- Taylor, K. M., Morgan, H. E., Johnson, A., and Nicholson, R. I. (2005). Structure-function analysis of a novel member of the LIV-1 subfamily of zinc transporters. ZIP14. *FEBS Lett.* 579, 427–432. doi: 10.1016/j.febslet.2004.12.006
- Tuncay, E., Bilginoglu, A., Sozmen, N. N., Zeydanli, E. N., Ugur, M., Vassort, G., et al. (2011). Intracellular free zinc during cardiac excitation-contraction cycle: calcium and redox dependencies. *Cardiovasc. Res.* 89, 634–642. doi: 10.1093/cvr/cvq352
- Turan, B., Fliss, H., and Désilets, M. (1997). Oxidants increase intracellular free Zn<sup>2+</sup> concentration in rabbit ventricular myocytes. *Am. J. Physiol.* 272(5 Pt 2), H2095–H2106.
- Voigt, J.-U., Pedrizzetti, G., Lysyansky, P., Marwick, T. H., Houle, H., Baumann, R., et al. (2015). Definitions for a common standard for 2D speckle tracking echocardiography: consensus document of the EACVI/ASE/Industry Task Force to standardize deformation imaging. *Eur. Heart J. Cardiovasc. Imag.* 16, 1–11. doi: 10.1093/ehjci/jeu184
- Wallenborn, J. G., Evansky, P., Shannahan, J. H., Vallanat, B., Ledbetter, A. D., Schladweiler, M. C., et al. (2008). Subchronic inhalation of zinc sulfate induces cardiac changes in healthy rats. *Toxicol. Appl. Pharmacol.* 232, 69–77. doi: 10.1016/j.taap.2008.05.025
- Wang, L., Zhou, Z., Saari, J. T., and Kang, Y. J. (2005). Alcohol-induced myocardial fibrosis in metallothionein-null mice. *Am. J. Pathol.* 167, 337–344. doi: 10.1016/s0002-9440(10)62979-3
- Wu, H., Li, L., Niu, P., Huang, X., Liu, J., Zhang, F., et al. (2017). The structure-function remodeling in rabbit hearts of myocardial infarction. *Physiol. Rep.* 5:e13311. doi: 10.14814/phy2.13311

**Conflict of Interest:** The authors declare that the research was conducted in the absence of any commercial or financial relationships that could be construed as a potential conflict of interest.

Copyright © 2021 Li, Niu, Wang, Bing, Tan and Huo. This is an open-access article distributed under the terms of the Creative Commons Attribution License (CC BY). The use, distribution or reproduction in other forums is permitted, provided the original author(s) and the copyright owner(s) are credited and that the original publication in this journal is cited, in accordance with accepted academic practice. No use, distribution or reproduction is permitted which does not comply with these terms.